CHEMISTRY
A European Journal

A Journal of ChemPubSoc Europe

Accepted Article

Title: Peroxidase-Mimicking Nanozyme with Enhanced Activity and High Stability based on Metal-Support Interaction

Authors: Zhihao Li, Xiangdong Yang, Yanbing Yang, Yaning Tan, Yue He, Meng Liu, Xinwen Liu, and Quan Yuan

To be cited as: *Chem. Eur. J.* 10.1002/chem.201703833

Link to VoR: http://dx.doi.org/10.1002/chem.201703833

Supported by ACES

WILEY-VCH

Peroxidase-Mimicking Nanozyme with Enhanced Activity and High Stability based on Metal-Support Interaction

Zhihao Li, Xiangdong Yang, Yanbing Yang, Yaning Tan, Yue He, Meng Liu, Xinwen Liu, Quan Yuan* [a]

Abstract: Peroxidase-mimicking nanozyme offers unique advantages of high stability and low cost over natural peroxidase for applications in bioanalysis, biomedicine and pollution treatment. However, the design of high-efficiency peroxidase-mimicking nanozymes remains a grand challenge. In this work, we adopted a structural design approach through hybridization of cube-CeO_2 and Pt nanoparticles to create a novel peroxidase-mimicking nanozyme with high efficiency and excellent stability. Compared to pure cube-CeO_2 and Pt nanoparticles, the as-hybridized Pt/cube-CeO_2 nanocomposites display much improved activity because of the strong metal-support interaction. Meanwhile, the nanocomposites also maintain high catalytic activity after long-term storage and several-time recycle. Based on their excellent properties, Pt/cube-CeO_2 nanocomposites were used to construct high-performance colorimetric biosensors for the sensitive detection of metabolites including H_2O_2 and glucose. Our findings highlight opportunities for the development of high-efficiency peroxidase-mimicking nanozyme with potentially various applications in diagnostic, biomedicine and pollution treatment.

Introduction

Enzymes carry out a host of biochemical reactions in living things.[1] Up to date, natural enzymes have been extensively studied in various areas such as fundamental research, biomedicine and biosensing due to their extraordinary substrate specificity and fascinating catalytic efficiency.[2,3] However, they generally suffer from several drawbacks such as inherent intolerance to harsh conditions and ease of denaturation, seriously limiting their large-scale applications.[2–5] To circumvent these limitations, substantial efforts have been channeled toward creating enzyme mimetics over the past decades. Driven by the rapid development of nanotechnology, numerous nanozymes with enzyme-mimicking properties have been discovered and received increasing attention recently because of their high stability and robustness while compared to enzymes.[6–9] Meanwhile, the distinct advantages of large surface area, tunable catalytic activities, ease to synthesize, as well as low costs, promise nanozyme as a viable alternative to natural enzymes.[10–12] To date, nanozymes have been demonstrated to display mimetic activities of diverse natural enzymes including catalase[13,14], peroxidase[15–17], oxidase[18,19] and phosphatase[20]. Among them, peroxidase-mimicking nanozymes which can catalyze the decomposition of peroxides and the oxidation of certain substrates, have entered the market with fast growing rate for enormous potential applications in medical diagnostics and disease therapy.[21-24] For instance, they are known to play important roles in detoxifying hydrogen peroxide and maintaining the oxidative balance in biological systems. In addition, peroxidase-mimicking nanozymes are capable of catalyzing color reactions and can be utilized to construct biosensors for applications in detection and imaging. In spite of the opportunities, it remains highly desirable but challenging to develop novel peroxidase-mimicking nanozymes with high efficiency.

In recent years, oxide-based nanocomposites are emerging as promising materials for highly efficient catalysts because the interaction between oxide and other components often results in an improved catalytic performance.[25–27] Particularly, cerium oxide (CeO_2), one of the most attractive rare-earth oxides, has been a significant active component of nanocomposites because of its high oxygen storage capacity and excellent catalytic activity.[28–30] CeO_2 has a mixed oxidation state (Ce^{3+}, Ce^{4+}), and exhibits strong redox behavior by switching between these two states, which is analogous to the catalytic cycle of natural redox enzymes.[31,32] As such, CeO_2 has been reported to display mimetic properties of multi-enzymes including peroxidase.[33,34] In this regard, rational design of CeO_2-based nanocomposites can provide a highly promising strategy to enhance the overall catalytic performance, and thus develop a new candidate of high-efficiency peroxidase-mimicking nanozymes.

Herein, we constructed a high-efficiency peroxidase-mimicking nanozyme based on the hybrid of CeO_2 nanocubes (cube-CeO_2) and platinum (Pt) nanoparticles. Pt nanoparticle is demonstrated to be an excellent antioxidant that can scavenge peroxides, resembling the activities of peroxidase.[35] Moreover, the introduction of Pt nanoparticle contributes to a strong interaction between two components, which can dramatically improve the catalytic activity of nanocomposites.[36,37] As a result, this designed nanozyme, termed as Pt/cube-CeO_2 nanocomposite, exhibits remarkably enhanced peroxidase-mimicking activity over pure cube-CeO_2 and Pt nanoparticles. In addition, the Pt/cube-CeO_2 nanocomposite exhibits high long-term stability and reusability. The enhanced activity and high stability enabled the Pt/cube-CeO_2 nanocomposite to construct high-performance biosensors for the colorimetric detection of H_2O_2 and glucose. Our demonstration of Pt/cube-CeO_2 nanocomposite provides a vivid example to develop high-efficiency and high-stability nanozymes for a variety of applications in various fields including bioanalysis, biomedicine and environmental protection.

Results and Discussion

The synthetic approach for preparing the Pt/cube-CeO_2 nanocomposites is illustrated in Scheme 1. The original CeO_2 nanoparticles stabilized with oleic acids (designed as cube-CeO_2-COOH) were synthesized by a facile hydrothermal method reported

[a] *Z. Li, X. Yang, Y. Yang, Y. Tan, Y. He, M. Liu, X. Liu, Prof. Q.Yuan*
Key Laboratory of Analytical Chemistry for
Biology and Medicine (Ministry of Education)
College of Chemistry and Molecular Sciences
Wuhan University, Wuhan 430072 (P.R. China)
E-mail: yuanquan@whu.edu.cn

Supporting information for this article is given via a link at the end of the document.

10.1002/chem.201703833

WILEY-VCH

previously[38] (see details in Experimental Section). For further decoration of Pt nanoparticles, the as-synthesized oil-dispersed cube-CeO_2-COOH nanoparticles were functionalized with PEI to transfer to aqueous phase and alter the surface charges. Subsequently, Pt nanoparticles were directly immobilized onto the surface of cube-CeO_2-NH_2 nanoparticles *via* a polyol reduction process described by Kim *et al.*[39], in which ethylene glycol (EG) and H_2PtCl_6 act as reduction agent and Pt precursor, respectively. To be specific, the alcohol groups of EG are oxidized to aldehydes and carboxyl acids, and at the same time, the electrons donated from EG trigger the reduction of $PtCl_4^{2-}$ which was absorbed at the surface of cube-CeO_2-NH_2 nanoparticles *via* electrostatic interaction.

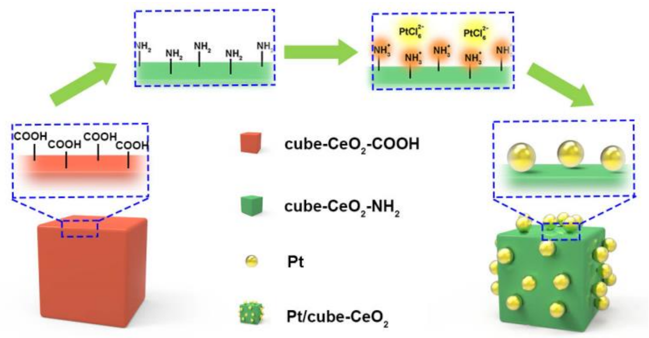

Scheme 1. Schematic illustration of the synthesis process of the Pt/cube-CeO_2 nanocomposites.

The functionalization of cube-CeO_2 nanoparticles were confirmed by Fourier Transformed infrared (FTIR) spectroscopy (Figure S1). For oleic acid-cappd cube-CeO_2-COOH nanoparticles, the characteristic peak at 1550 cm^{-1} and 1430 cm^{-1} were assigned to the in-plane bending vibration of =C–H in the oleic acid molecules. After PEI functionalization, cube-CeO_2-NH_2 nanoparticles display two bands around 1650 cm^{-1} and 1380 cm^{-1} which are assigned to the bending and vibration of N–H. Additionally, zeta potential analysis indicates that cube-CeO_2-NH_2 nanoparticles have a positive charge of +36 mV (Figure S2), indicating that the amino groups have been successfully introduced into the cube-CeO_2-NH_2 nanoparticles. Transmission electron microscopy (TEM) was performed to investigate the morphology and structure of the as-prepared Pt/cube-CeO_2 nanocomposites. Figure S5 shows the TEM image of cube-CeO_2-NH_2 nanoparticles. Evidently, these nanoparticles display excellent monodispersity and highly uniform in cubic shape with an average size of 6 nm. After functionalization with Pt, spherical shaped nanoparticles with uniform distribution and an average size of 2 nm can be seen clearly around the cube-CeO_2 as depicted in Figure 1a, revealing the successful growth of Pt nanoparticles on the surface of cube-CeO_2 nanoparticles. Moreover, the well-defined crystalline fringe with interplanar spacing of 0.32 nm in the cube-CeO_2 is consistent with the d spacing of the (111) plane of cube-CeO_2. Figure 1b shows the XRD pattern of the cube-CeO_2 nanoparticles and Pt/cube-CeO_2 nanocomposites. The as-prepared cube-CeO_2 nanoparticles exhibit a series of characteristic peaks which correspond to a typical cubic fluorite CeO_2 crystal phase (JCPDS No. 34-0394). In comparison, an extra characteristic peak at $2\theta = 32.5°$ which is assigned to the (111) crystal plane of Pt nanoparticles appears in the Pt/cube-CeO_2 nanocomposites, indicating that well-crystallized Pt nanocrystals were successfully included in the nanocomposites. Based on the above results, it can be concluded that the well-defined Pt/cube-CeO_2 nanocomposites with superior dispersity and high uniformity were successfully fabricated.

To validate the peroxidase-mimicking activity of Pt/cube-CeO_2 nanocomposites, a typical colorimetric reaction was carried out with TMB as a chromogenic substrate. The mechanism of this reaction is schematically illustrated in Figure 2a. Specifically, in the presence of H_2O_2, Pt/cube-CeO_2 nanocomposites can simultaneously catalyze

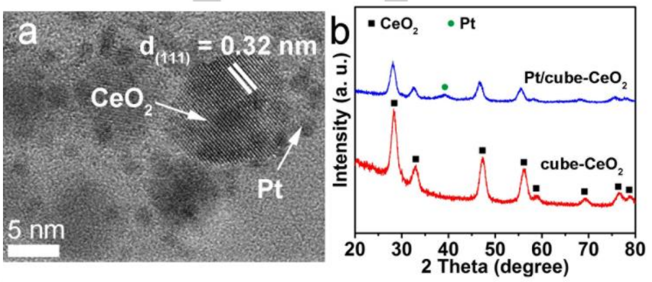

Figure 1. (a) TEM image of Pt/cube-CeO_2 nanocomposites (b) XRD pattern of the Pt/cube-CeO_2 nanocomposites and cube-CeO_2 nanoparticles.

the degradation of H_2O_2 to O_2 and the oxidation of TMB to oxTMB which is a blue-colored product. An absence experiment was performed to verify the necessary components for the catalytic reaction as shown in Figure 2b. In the absence of Pt/cube-CeO_2 nanocomposites or H_2O_2, the absorbance at 650 nm displays negligible change and the reaction solution remains transparent and clear, indicating that nanocomposites or H_2O_2 alone cannot catalyze the generation of oxTMB. On the other hand, when Pt/cube-CeO_2 nanocomposites and H_2O_2 were both present in the system, a strong absorbance at 650 nm emerges and the color of the solution immediately changes to blue, suggesting that TMB was oxidized to oxTMB only in the synchronous presence of both nanocomposites and H_2O_2. At the same time, time-dependent absorbance changes of the three different systems were measured to record the reaction process. As depicted in Figure S8, absorbance of the system with only H_2O_2 or Pt/cube-CeO_2 nanocomposites remains at the original value over the whole reaction process, while absorbance of the solution with nanocomposites and H_2O_2 rapidly increases to a high value at the initial 10 min and then slowly saturates after 25 min reaction. As the reaction proceeds, UV-vis absorption spectra of the solution containing nanocomposites and H_2O_2 clearly reveals the successively increase of absorbance (Figure 2c). To further confirm the generality of catalytic activity of Pt/cube-CeO_2 nanocomposites, another substrate 2,2‘-azino-bis(3-ehtylbenzothiazoline) (ABTS) was used to test the catalytic activity of Pt/cube-CeO_2 nanocomposites and similar results were obtained as shown in Figure S9. The findings from all the experiments above demonstrate that Pt/cube-CeO_2 nanocomposites exhibit a peroxidase-mimicking behavior toward typical peroxidase substrates.

In order to further investigate the peroxidase-like activity of Pt/cube-CeO_2 nanocomposites, steady-state kinetics analysis was

10.1002/chem.201703833

WILEY-VCH

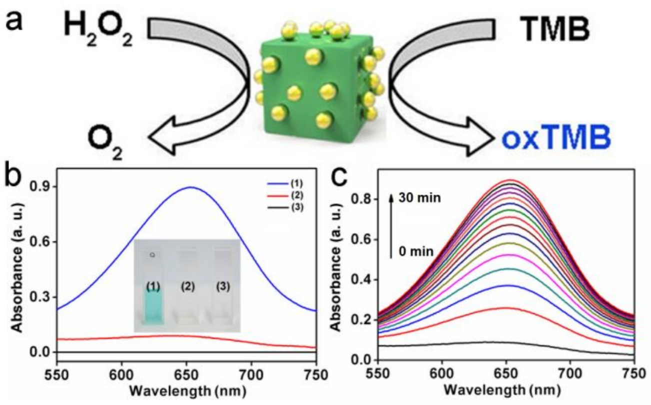

Figure 2. (a) Schematic drawing of TMB oxidation in the presence of H_2O_2 using Pt/cube-CeO_2 nanocomposites as peroxidase-mimicking nanozymes. (b) UV-vis absorption spectra of different reaction solutions with (1) Pt/cube-CeO_2 nanocomposites and H_2O_2, (2) H_2O_2 only and (3) Pt/cube-CeO_2 nanocomposites only. Insets are the corresponding photograph of different reaction solutions. (c) Time-dependent UV-vis absorption spectra of the catalytic system with TMB as substrate in the presence of both Pt/cube-CeO_2 nanocomposites and H_2O_2.

performed using the enzyme kinetic model[7,8]. In the kinetic assays, the concentration of Pt/cube-CeO_2 nanocomposites used for TMB oxidation was kept at 10 μg mL^{-1}. As shown in Figure 97a, with varied TMB concentration from 0.05 mM to 0.6 mM and fixed H_2O_2 concentration at 0.05 mM, the reaction catalyzed by Pt/cube-CeO_2 nanocomposites shows a typical Michaelis-Menten kinetics[7,8]. A similar result was observed when TMB concentration was fixed at 0.1 mM and H_2O_2 concentration was varied from 0.05 mM to 0.5 mM as depicted in Figure S10b. Then, the Michaelis-Menten curve of TMB was fitted to Lineweaver-Burk plot[40,41] as Figure S10c shows and Lineweaver-Burk plot of H_2O_2 was obtained in a similar way as presented in Figure S10d. According to the plots, the Michaelis-Menten constant (K_m) and the maximum reaction velocity (V_{max}) were calculated to quantatively evaluate the catalytic activity of enzymes as listed in Table S1. Here, K_m is recognized as an important indicator to assess the affinity between nanozyme and substrates, with a small K_m value representing a strong affinity to substrates. The K_m value of Pt/cube-CeO_2 nanocomposites with H_2O_2 as substrate (0.21 mM) was much lower than that of horseradish peroxidase (HRP, 3.70 mM). The K_m value with TMB (0.26 mM) was lower than that of HRP (0.43 mM). These results indicate that the Pt/cube-CeO_2 nanocomposites exhibit strong binding affinity to substrates. In addition, the V_{max} value of Pt/cube-CeO_2 nanocomposites with TMB as substrate was calculated as 1.47 10^{-7} M s^{-1}, which is found to be comparable to that of HRP (1.00 10^{-7} M s^{-1}). A comparable V_{max} value (0.85 10^{-7} M s^{-1}) with H_2O_2 as substrate was also calculated compared to that of HRP (0.87 10^{-7} M s^{-1}). The K_m and V_{max} values of Pt/cube-CeO_2 nanocomposite were also compared with other nanozymes. As listed in Table S2, compared to most of other nanozymes, the K_m values of Pt/cube-CeO_2 nanocomposites were smaller, indicating that Pt/cube-CeO_2 nanocomposites exhibit strong affinity to substrates. Besides, the V_{max} values of Pt/cube-CeO_2 nanocomposites are comparable to other nanozymes. All the results above demonstrate that Pt/cube-CeO_2 nanocomposites exhibit excellent catalytic activity.

Next, the peroxidase-mimicking activities of Pt/cube-CeO_2 nanocomposite, cube-CeO_2 nanoparticles and Pt nanoparticles were investigated. As shown in Figure 3a, in the presence of TMB and H_2O_2, the solution containing individual cube-CeO_2-NH_2 nanoparticles shows little color change as well as negligible absorbance variation at 650 nm. A similar result was obtained in the solution containing Pt nanoparticles. In addition, it was clearly observed that the solution containing both cube-CeO_2 and Pt nanoparticles also displays little absorbance variation and negligible color change. In contrast, the system containing Pt/cube-CeO_2 nanocomposites shows a remarkable absorbance variation and the color of the reaction solution immediately changes to deep blue in a short time. These findings demostrate that the designed Pt/cube-CeO_2 nanocomposites exhibit improved catalytic activity.

In the previous works, numerous noble metal-ceria nanocomposites including Au/CeO_2[42], Pt/CeO_2[43] and Pd/CeO_2[29], have been reported to exhibit enhanced catalytic activity. A lot of experiments, characterizations and calculations[42–44] were carried out to understand the interaction between noble metal and ceria, which was proposed as metal-support interaction[43]. Recently, Pt/ceria nanocomposite has been demonstrated to be a highly efficient catalyst for carbon dioxide reforming of methane and the

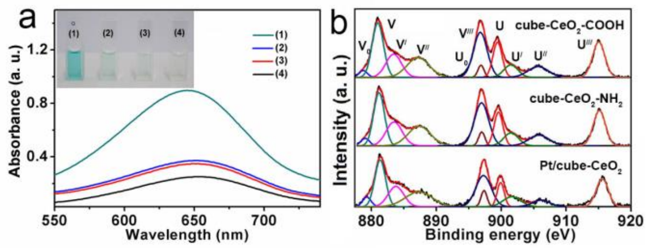

Figure 3. (a) UV-vis absorption spectra of different reaction solutions with (1) Pt/cube-CeO_2 nanocomposites, (2) the mixture of Pt and cube-CeO_2 nanoparticles, (3) Pt nanoparticles alone, and (4) cube-CeO_2 nanoparticles alone as catalysts. Insets are the corresponding photographs of different reaction solutions. (b) High-resolution XPS spectra of the Ce 3d for the cube-CeO_2-COOH nanoparticles, cube-CeO_2-NH_2 nanoparticles, and Pt/cube-CeO_2 nanocomposites.

high activity of the Pt/ceria nanocomposite can be explained by a Pt-support interaction.[45] To be specific, Pt nanoparticles would cause a change of the electronic states on the surface of CeO_2 nanoparticles and thus contribute to a shorter distance between oxygen atom and Pt atoms.[45] Consequently, the oxygen atom is readily reduced, and at the same time, Ce^{4+} is easily transferred to the low oxidation state of Ce^{3+}, resulting in an increased ratio of Ce^{3+}/Ce^{4+}.[45] Besides, previous reports[24,46] have demonstrated that a higher Ce^{3+}/Ce^{4+} ratio is related to an enhanced peroxidase-mimicking activity of ceria-based nanozymes. X-ray photoelectron spectra (XPS) was recorded to analyze the surface Ce chemical states of different nanoparticles including cube-CeO_2-COOH, cube-CeO_2-NH_2 and Pt/cube-CeO_2. As indicated in Figure 4b, the characteristic peaks of Ce 3d XPS spectra are divided into two groups, V_0, V′, U_0, U′ for Ce^{3+} and V, V′′,V′′′, U, U′, U′′′ for Ce^{4+}. Then, the Ce^{3+}/Ce^{4+} ratio of cube-CeO_2-COOH nanoparticles, cube-CeO_2-NH_2 nanoparticles, and Pt/cube-CeO_2 nanocomposites were calculated according to the XPS spectra and the results are compared as presented in Table 1.

10.1002/chem.201703833

From the table, it can be seen that among the three systems, the Pt/cube-CeO_2 nanocomposites show the highest Ce^{3+}/Ce^{4+} ratio. On the basis of these models and results, the enhanced peroxidase-mimicking activity of Pt/cube-CeO_2 nanocomposites is probably ascribed to the strong interaction between Pt and cube-CeO_2. To further explore the effect of Pt on the peroxidase-mimicking activity of nanocomposites, the Pt/cube-CeO_2 nanocomposites with different Pt contents were synthesized and their activities were compared. As depicted in Figure S12, a remarkable increase of peroxidase-mimicking activity is observed as the concentration of Pt precursor solutions used for the synthesis of Pt/cube-CeO_2 nanocomposites ranging from 19.3 μM to 145 μM. When the concentration of Pt precursor solution increases to more than 145 μM, the catalytic activity of nanocomposites gradually decreases. A previous work has demonstrated that the aggregation of Pt nanoparticles can reduce the effective reactive sites and lead to a decrease in catalytic activity.[47] Accordingly, the decreased catalytic activity in the case of Pt/cube-CeO_2 nanocomposites at high Pt content can be explained by the aggregation of Pt nanoparticles. Based on the above results, we can infer that Pt/cube-CeO_2 nanocomposites exhibit enhanced peroxidase-mimicking activity due to strong metal-support interaction and that the content of Pt has a significant impact on the catalytic activity of Pt/cube-CeO_2 nanocomposites.

Table 1. The percentage of Ce^{3+} and Ce^{4+} in the cube-CeO_2-COOH, cube-CeO_2-NH_2, Pt/cube-CeO_2.

	Ce^{3+} / (Ce^{3+} + Ce^{4+}) (%)	Ce^{4+} / (Ce^{3+} + Ce^{4+}) (%)
cube-CeO_2-COOH	20.1	79.9
cube-CeO_2-NH_2	25.2	74.8
Pt/cube-CeO_2	28.9	71.1

Stability is one of the most important properties for catalysts.[48] Due to their protein or RNA nature, natural enzymes are easy of inactivation in surrounding environments and suffer from poor stability.[4,5] The insufficient stability of natural enzyme not only limits the lifetime of enzyme-based biosensors and bioreactors,[49] but also leads to high cost in production and storage of enzymes.[50] Therefore, a catalyst with high stability and a long shelf life is of great importance. To evaluate the stability of Pt/cube-CeO_2 nanocomposite, the long-term stability and reusability were investigated. To investigate the long-term stability, the Pt/cube-CeO_2 nanocomposite was kept at room temperature and its catalytic activity was measured during a two-week period as presented in Figure 4a. It can be observed that after two weeks, Pt/cube-CeO_2 nanocomposites exhibit only a slight decrease in catalytic activity, indicating that the Pt/cube-CeO_2 nanocomposite is easy to storage and possess excellent long-term stability. In addition, the Pt/cube-CeO_2 nanocomposites were collected by centrifugation after each reaction, washed with water twice and redispersed into water for reuse. The peroxidase-mimicking activity of each cycle was measured as presented in Figure 4b. After 6 cycles, the catalytic activity of the nanocomposites remained over 90% with only a little decrease. The slight decay in activity may be ascribed to the loss of nanocomposites during centrifugation. According to the above investigations, the Pt/cube-CeO_2 nanocomposites display excellent long-term stability as well as high reusability, and hold great promise in practical applications.

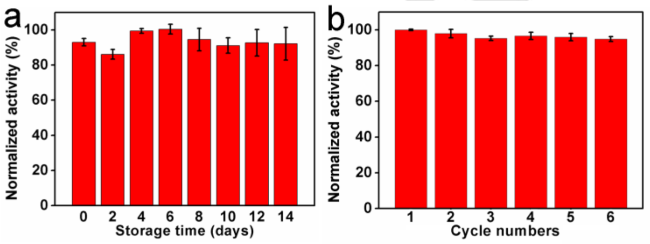

Figure 4. Catalytic activity of the Pt/cube-CeO_2 nanocomposites with (a) different storage time and (b) different cycle numbers.

The as-synthesized Pt/cube-CeO_2 nanocomposites were used to construct biosensors for colorimetric detection of H_2O_2 and glucose. H_2O_2 is an important signalling molecule and is involved in a variety of vital processes such as inflammation, immune and tumorigenesis.[51] Based on the peroxidase-mimicking properties of Pt/cube-CeO_2 nanocomposites, the quantitative determination of H_2O_2 using the nanocomposites is demonstrated as Figure 5 presents. Figure 5a depicts the UV-vis absorption spectra of the reaction solutions with different concentrations of H_2O_2. As the H_2O_2 concentration increases, the absorbance of the reaction solutions shows a successively increase. Meanwhile, color of the solution with different H_2O_2 concentration changes from colorless to deep blue due to the amplified TMB oxidation (Figure S13), indicating that this biosensor based on Pt/cube-CeO_2 nanocomposites can be successfully used for visual determination of H_2O_2. Furthermore, absorbance at 650 nm as a function of H_2O_2 concentration is plotted in Figure 5b and the inset shows the initial linear response of the biosensor. According to the curve, it can be calculated that the limit of detection (LOD) for H_2O_2 was as low as 10.7 μM. All the above results suggest that the Pt/cube-CeO_2 nanocomposites can be used to construct sensitive biosensors for colorimetric detection of H_2O_2.

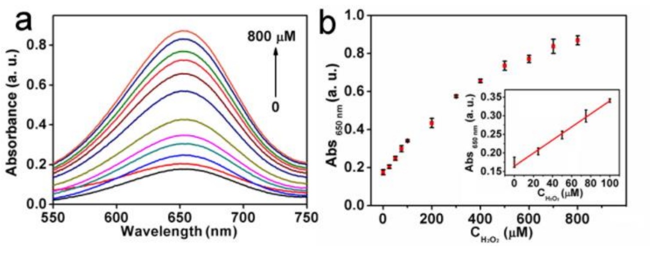

Figure 5. (a) UV-vis absorption spectra of the reaction systems with the Pt/cube-CeO_2 nanocomposites-based biosensor for the detection of H_2O_2. The H_2O_2 concentration was 0, 25, 50, 75, 100, 200, 300, 400, 500, 600, 700, and 800 μM. (b) Absorbance at 650 nm as a function of H_2O_2 concentration. Inset is the initial linear response of the Pt/cube-CeO_2 nanocomposites-based biosensor.

Glucose is the most important energy source in biosystems and the fluctuation of glucose concentration is often associated with many diseases such as diabetes, cancer, and neurological disorders.[52] Based on the fact that the Pt/cube-CeO_2

10.1002/chem.201703833

nanocomposites exhibit superior activity for the detection of H_2O_2, a colorimetric glucose biosensor based on Pt/cube-CeO_2 nanocomposites was developed. The design principle of glucose biosensor is outlined in Figure 6a. Specifically, the glucose oxidase catalyzes the oxidation of glucose to generate H_2O_2 in the presence of dissolved O_2. As the H_2O_2 forms, the Pt/cube-CeO_2 nanocomposites can subsequently catalyze the oxidation of TMB to oxTMB. The formed oxTMB can produce a strong absorbance at 650 nm as Figure 6b shows. The absorbance of the reaction solution exhibits an obvious increase with the increase of glucose concentration, which is consistent with the absorption variations in Figure S14. As depicted in the inset of Figure 6b, it can be observed that the linear response is in the range of 0 to 100 μM, and the calculated LOD is 4.1 μM. At the same time, the corresponding photographs of the reaction solutions with different glucose concentrations were presented in Figure S15. It can be clearly seen that the colour of the solution changes from colourless to light blue and then gradually turns deep blue with the increase of glucose concentration, indicating that the glucose can be directly read out by naked eyes. Furthermore, the selectivity of the Pt/cube-CeO_2 nanocomposites-based biosensor was investigated. As indicated in Figure 6c, the introduction of glucose analogues such as fructose, mannose, galactose, sucrose and maltose with a high concentration of 1 mM into the reaction system just generate a negligible absorption variation. On the contrast, the reaction system with glucose results in a considerable absorbance variation even with a much lower concentration, demonstrating that the Pt/cube-CeO_2 nanocomposites-based biosensor exhibits high selectivity towards glucose. These results indicated that the Pt/cube-CeO_2 nanocomposites can be utilized to construct biosensors for the colorimetric detection of H_2O_2 and glucose with good sensitivity and selectivity.

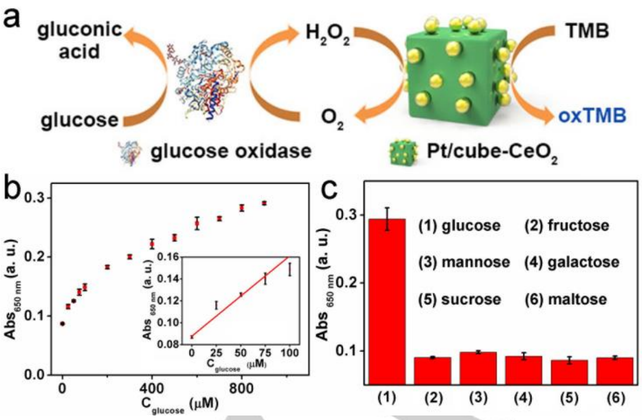

Figure 6. (a) Schematic drawing for the detection of glucose using the Pt/cube-CeO_2 nanocomposites-based biosensor. (b) Absorbance at 650 nm as a function of glucose concentration. The concentration of glucose solution was 0, 25, 50, 75, 100, 200, 300, 400, 500, 600, 700, 800, and 900 μM. Inset is the initial response of the Pt/cube-CeO_2 nanocomposites-based biosensor. (c) Selectivity assays for glucose detection. The concentrations of glucose, fructose, mannose, galactose, sucrose and maltose are all kept at 1 mM.

Conclusions

In conclusion, we designed a high-performance peroxidase-mimicking nanozyme based on Pt/cube-CeO_2 nanostructure. Compared to pure cube-CeO_2 and Pt nanoparticles, the Pt/cube-CeO_2 nanocomposite exhibits a higher catalytic efficiency because of the metal-support effect between cube-CeO_2 and Pt nanoparticles. In addition, this nanocomposite possesses good long-term stability and reusability. Based on these excellent properties, Pt/cube-CeO_2 nanocomposite-based biosensors were constructed and used for the sensitive and selective colorimetric detection of metabolites including H_2O_2 and glucose. This nanocomposite provides a new strategy to construct high-efficiency peroxidase-mimicking nanozymes based on the metal-support effect for applications in medical diagnostic and therapy.

Experimental Section

Chemicals

Oleic acid (OA), oleylamine (OM, 80% ~ 90%), cyclohexane (>99%), ethanol (AR), dimethyl sulfoxide (DMSO, AR), sodium dodecyl sulfate (SDS), chroloplatinic acid (H_2PtCl_6•$6H_2O$, AR), sodium chloride (>99.8%), sodium acetate (>99%), acetic acid (>99.5%), sodium hydroxide (>96%), ethylene glycol (>99%), hydrogen peroxide (H_2O_2, 30 %) and 3, 3′, 5, 5′-tetramethylbenzidine (TMB, >99%) were purchased from Sinopharm Chemical Reagent Co. (China). Ammonium cerium nitrate ($(NH_4)_2Ce(NO_3)_6$, >99%), glucose oxidase (GOx), horseradish peroxidase (HRP), 2,2'-azino-bis(3-ehtylbenzothiazoline) (ABTS) and polyethyleneimine (PEI) were purchased from Sigma Aldrich.

Synthesis of cube-CeO_2-COOH nanoparticles

Oleic acid capped cube-CeO_2 (designated as cube-CeO_2-COOH) nanoparticles were synthesized according to a previously reported method.[37] Briefly, 0.5482 g of $(NH_4)_2Ce(NO_3)_6$ and 9.7 mL of oleylamine were added into a flask and heated to 110 °C with vigorous stirring. Then, 3.2 mL of oleic acid was added to the above transparent solution under stirring at room temperature. Next, the mixed solution was transferred to a Teflon bottle containing 50 mL water and 0.0136 g sodium dodecyl sulfate (SDS). After stirring at room temperature for 30 min, the resultant slurry was transferred into a steel autoclave. Subsequently, the system was heated to 220 °C and kept for 24 h. After cooling to room temperature, the obtained products were separated by centrifugation, and then purified by washing with cyclohexane and ethanol for three times.

Preparation of cube-CeO_2-PEI nanoparticles

5 mg of cube-CeO_2-COOH nanoparticles were dispersed into 20 mL of dimethyl sulfoxide (DMSO) through ultrasonic treatment and then heated to 95 °C. Subsequently, 10 mL of DMSO with 0.1 g polyethyleneimine (PEI) was added into the slurry and kept at 95 °C for 4 h. After cooling down to room temperature, the as-obtained PEI-functionalized cube-

CeO_2 (designated as cube-CeO_2-NH_2) nanoparticles were obtained by centrifugation and washed with deionized water for three times.

Synthesis of Pt/cube-CeO_2 nanocomposites

The as-prepared cube-CeO_2-NH_2 nanoparticles were redispersed into 2 mL deionized water and 22.5 mL ethylene glycol with ultrasonic for 15 min. Subsequently, the H_2PtCl_6 solution (19.3 mM) with different volumes of 25 μL, 50 μL, 75 μL and 100 μL were separately added into the above mixture solution under ultrasonic to give Pt/cube-CeO_2 nanocomposites with different Pt contents. The resultant solution was then transferred into a three-necked bottle, followed by addition of 100 μL of NaOH solution (0.07 g mL^{-1}) under stirring. Different volume of water was added into the solution to keep the total volume at 25 mL. Subsequently, the mixture was heated to 140 °C and refluxed for 2.5 h. Finally, the nanocomposites were recovered by centrifugation and washed with water for three times. SiO_2 nanoparticles were synthesized according to a previously reported method[53]. Briefly, CTAB (1 g) and NaOH aqueous solution (2 M, 3.50 mL) were added into a bottle containing 480 mL water. Next, the mixture was heated to 85 °C and TEOS (22.4 mmol, 5 mL) was added, followed by stirring for 2 h. The solid product was filtered and washed with methanol. For –NH_2 modification, 25 mg SiO_2 was dispersed in 25 mL isopropyl alcohol and heated to 85 °C, followed by the addition of 100 μL 3-aminopropyltriethoxysilane. Finally, SiO_2–NH_2 nanoparticles were obtained after reaction for 6 h. Pt/SiO_2 was synthesized in a similar way to the fabrication of Pt/cube-CeO_2 nanocomposites.

Peroxidase-like catalytic activity of Pt/cube-CeO_2 nanocomposites

Typically, the peroxidase-like catalytic reaction based on Pt/cube-CeO_2 nanocomposites was carried out at 25 °C with 100 μL of 0.1 mg mL^{-1} Pt/cube-CeO_2 nanocomposites, 50 μL of 1 mM 3, 3′, 5, 5′-tetramethylbenzidine (TMB) and 100 μL of 1 mM H_2O_2 successively added into 750 μL of acetate buffer (0.05 M, pH = 4.0), unless otherwise stated. The absorbance at 650 nm after 30 min reaction or the absorbance variation at 650 nm within 25 min was measured by a UV-vis spectrophotometer.

Steady-state kinetic analysis of Pt/cube-CeO_2 nanocomposites

All the kinetic assays were conducted at room temperature in a UV-vis cell. Specifically, 750 μL of acetate buffer (0.05 M, pH = 4.0) and 100 μL of 0.1 mg mL^{-1} c-CeO_2/Pt nanocomposites were mixed into the cell followed by addition of 50 μL of TMB and 100 μL of H_2O_2 with certain concentrations. After addition of substrates, the absorbance changes at 650 nm were immediately measured with an interval of 5 seconds for 3 min. The assays using TMB as substrate were conducted with fixed H_2O_2 concentration of 1 mM and varied TMB concentration from 1 mM to 12 mM. Kinetic analysis with H_2O_2 as substrate was carried out in a similar way as TMB by fixing TMB concentration at 1 mM and varying H_2O_2 concentration from 0.5 mM to 5 mM. The kinetic parameters were calculated from Michaelis-Menten equation: $1/V = K_m / V_{max}(1/[S] + 1/K_m)$, where V represents the initial rate, K_m is the Michaelis constant, V_{max} corresponds to the maximal reaction velocity and $[S]$ is the concentration of substrate.

Detection of H_2O_2 and glucose

For H_2O_2 detection, 750 μL of acetate buffer (0.05 M, pH = 4.0) solution, 50 μL of 1 mM TMB and 100 μL of 0.1 mg mL^{-1} c-CeO_2/Pt nanocomposites were mixed in a tube followed by addition of 100 μL H_2O_2 solution with a certain concentration. After 30 min reaction, the absorbance of the reaction solution at 650 nm was measured by a UV-vis spectrophotometer. Glucose detection was carried out as follows: 20 μL of 1000 U mL^{-1} glucose oxidase, 100 μL of 0.1 mg mL^{-1} c-CeO_2/Pt nanocomposites, 50 μL of 1 mM TMB and 530 μL of acetate buffer (0.05 M, pH = 4.0) were thoroughly mixed in a tube. Then, 300 μL glucose solution with a certain concentration was added into the mixed solution and reacted for 1 h. Then, the absorbance at 650 nm was measured to quantify the glucose concentration.

Acknowledgements

This work was supported by the National Natural Science Foundation of China (21422105, 21675120), the National Key Research and Development Program of China (2017YFA0208000), the Natural Science Foundation of Hubei Province (2015CFA032) and Ten Thousand Talents Program for Young Talents. Q. Yuan thanks the large-scale instrument and equipment sharing foundation of Wuhan University.

Keywords: peroxidase-mimicking nanozyme • enhanced activity • nanocomposite • metal-support interaction • colorimetric detection

[1] M. Garcia-Viloca, J. Gao, M. Karplus, D. G. Truhlar, *Science* **2004**, *303*, 186–195.
[2] P. Dydio, H. M. Key, A. Nazarenko, J. Y. -E. Rha, V. Seyedkazemi, D. S. Clark, J. F. Hartwig, *Science* **2016**, *354*, 102–106.
[3] Y. Lin, J. Ren, X. Qu, *Acc. Chem. Res.* **2014**, *47*, 1097–1105.
[4] H. Wei, E. Wang, *Chem. Soc. Rev.* **2013**, *42*, 6060–6093.
[5] M. J. Wiester, P. A. Ulmann, C. A. Mirkin, *Angew. Chem. Int. Ed.* **2011**, *50*, 114–137.
[6] N. A. Kotov, *Science* **2010**, *330*, 188-189.
[7] L. Gao, J. Zhuang, L. Nie, J. Zhang, Y. Zhang, N. Gu, T. Wang, J. Feng, D. Yang, S. Perrett, X. Yan, *Nat. Nanotech.* **2007**, *2*, 577–583.
[8] R. Cai, D. Yang, S. Peng, X. Chen, Y. Huang, Y. Liu, W. Hou, S. Yang, Z. Liu, W. Tan, *J. Am. Chem. Soc.* **2015**, *137*, 13957–13963.
[9] W. Zhang, W. Lai, R. Cao, *Chem. Rev.* **2017**, *117*, 3717–3797.
[10] B. Liu, J. Liu, *Nano Res.* **2017**, *10*, 1125–1148.
[11] Y. Huang, Y. Lin, X. Ran, J, Ren, X. Qu, *Chem. Eur. J* **2016**, *22*, 5705–5711.
[12] H. Cheng, L. Zhang, J. He, W. Guo, Z. Zhou, X. Zhang, S. Nie, H. Wei, *Anal. Chem.* **2016**, *88*, 5489–5497.
[13] J. Fan, J. J. Yin, B. Ning, X. Wu, Y. Hu, M. Ferrari, G. J. Anderson, J. Wei, Y. Zhao, G. Nie, *Biomaterials* **2011**, *32*, 1611–1618.
[14] Z. Zhu, Z. Guan, S. Jia, Z. Lei, S. Lin, H. Zhang, Y. Ma, Z. Tian, C. Yang, *Angew. Chem. Int. Ed.* **2014**, *53*, 12503–12507; *Angew. Chem.* **2014**, *126*, 12711–12715.
[15] H. Liang, B. Liu, Q. Yuan, J. Liu, *ACS Appl. Mater. Interfaces* **2016**, *8*, 15615–15622.
[16] X. Wang, C. Hou, W. Qiu, Y. Ke, Q. Xu, X. Liu, Y. Lin, *ACS Appl. Mater. Interfaces* **2017**, *9*, 684–692.
[17] H. Sun, A. Zhao, N. Gao, K. Li, J. Ren, X. Qu, *Angew. Chem. Int. Ed.*

2015, *54*, 7176–7180; *Angew. Chem.* **2015**, *127*, 7282–7286.
[18] A. Asati, S. Santra, C. Kaittanis, S. Nath, J. M. Perez, *Angew. Chem. Int. Ed.* **2009**, *48*, 2308–2312; *Angew. Chem.* **2009**, *121*, 2344–2348.
[19] R. Pautler, E. Y. Kelly, O. J. J. Huang, J. Cao, B. Liu, J. Liu, *ACS Appl. Mater. Interfaces* **2013**, *5*, 6820–6825.
[20] M. H. Kuchma, C. B. Komanski, J. Colon, A. Teblum, A. E. Masunov, B. Alvarado, S. Babu, S. Seal, J. Summy, C. H. Baker, *Nanomed. - Nanotechnol.* **2010**, *6*, 738–744.
[21] X. Xia, J. Zhang, N. Lu, M. J. Kim, K. Ghale, Y. Xu, E. McKenzie, J. Liu, H. Ye, *ACS Nano* **2015**, *9*, 9994–10004.
[22] L. Su, J. Feng, X. Zhou, C. Ren, H. Li, X. Chen, *Anal. Chem.* **2012**, *84*, 5753–5758.
[23] Z. Yang, Y. Cao, J. Li, M. Lu, Z. Jiang, X. Hu, *ACS Appl. Mater. Interfaces* **2016**, *8*, 12031–12038.
[24] Z. Tian, J. Li, Z. Zhang, W. Gao, X. Zhou, Y. Qu, *Biomaterials* **2015**, *59*, 116–124.
[25] D. Wang, Z. Wang, P. Zhao, W. Zheng, Q. Peng, L. Liu, X. Chen, Y. Li, *Chem. Asian J.* **2010**, *5*, 925–931.
[26] L. Ma, D. Wang, J. Li, B. Bai, L. Fu, Y. Li, *Appl. Cata. B-Environ.* **2014**, *148*, 36–43.
[27] K. H. Park, Y. W. Lee, Y. Kim, S. W. Kang, S. W. Han, *Chem. Eur. J.* **2013**, *19*, 8053–8057.
[28] S. D. Senanayake, D. Stacchiola, J. Rodriguez, *Acc. Chem. Res.* **2013**, *46*, 1702–1711.
[29] X. Wang, Y. Zhang, S. Song, X. Yang, Z. Wang, R. Jin, H. Zhang, *Angew. Chem. Int. Ed.* **2016**, *55*, 4542–4546; *Angew. Chem.* **2016**, *128*, 4618–4622.
[30] Z. Liu, J. Wang, Y. Li, X. Hu, J. Yin, Y. Peng, Z. Li, Y. Li, B. Li, Q. Yuan, *ACS Appl. Mater. Interfaces* **2015**, *7*, 19416–19423.
[31] T. Pirmohamed, J. M. Dowding, S. Singh, B. Wasserman, E. Heckert, A. S. Karakoti, J. E. S. King, S. Seal, W. T. Self, *Chem. Commun.* **2010**, *46*, 2736–2738.
[32] E. G. Heckert, A. S. Karakoti, S. Seal, W. T. Self, *Biomaterials* **2008**, *29*, 2705–2709.
[33] B. Liu, Z. Sun, P. J. J. Huang, J. Liu, *J. Am. Chem. Soc.* **2015**, *137*, 1290–1295.
[34] Y. Lin, C. Xu, J. Ren, X. Qu, *Angew. Chem. Int. Ed.* **2012**, *51*, 12579–12583; *Angew. Chem.* **2012**, *124*, 12747–12751.
[35] X. Shen, W. Liu, X. Gao, Z. Lu, X. Wu, X. Gao, *J. Am. Chem. Soc.* **2015**, *137*, 15882–15891.
[36] G. N. Vayssilov, Y. Lykhach, A. Migani, T. Staudt, G. P. Petrova, N. Tsud, T. Skala, A. Bruix, F. Illas, K. C. Prince, V. Matolin, K. M. Neyman, J. Libuda, *Nat. Mater.* **2011**, *10*, 310–315.
[37] T. Yu, J. Zeng, B. Lim, Y. Xia, *Adv. Mater.* **2010**, *22*, 5188–5192.
[38] H. P. Zhou, H. S. Wu, J. Shen, A. X. Yin, L. D. Sun, C. H. Yan, *J. Am. Chem. Soc.* **2010**, *132*, 4998–4999.
[39] S. H. Park, H. N. Yang, D. C. Lee, K. W. Park, W. J. Kim, *Electrochim. Acta* **2014**, *125*, 141–148.
[40] M. Kluenker, M. N. Tahir, R. Ragg, K. Korschelt, P. Simon, T. E. Groelik, B. Barton, S. I. Shylin, M. Panthofer, J. Herzberger, H. Frey, V. Ksenofontov, A. Moller, U. Kolb, J. Grin, W. Tremel, *Chem. Mater.* **2017**, *29*, 1134–1146.
[41] K. Korschelt, R. Ragg, C. S. Metzger, M. Kluenker, M. Oster, B. Barton, M. Panthofer, D. Strand, U. Kolb, M. Mondeshki, S. Strand, J. Brieger, M. N. Tahir, W. Tremel, *Nanoscale* **2017**, *9*, 3952–3960.
[42] R. Si, M. F. Stephanopolous, *Angew. Chem. Int. Ed.* **2008**, *47*, 2884–2887; *Angew. Chem.* **2008**, *120*, 2926–2929.
[43] C. M. Y. Yeung, K. M. K. Yu, Q. J. Fu, D. Thompsett, M. I. Petch, S. K. Tsang, *J. Am. Chem. Soc.* **2005**, *127*, 18010–18011.
[44] M. Cargnello, V. V. T. D. Nguyen, T. R. Gordon, R. E. Diaz, E. A. Stach, R. J. Gorte, P. Fornasiero, C. B. Murry, *Science* **2013**, *341*, 771–773.
[45] Z. Zhang, J. Li, W. Gao, Y. Ma, Y. Qu, *J. Mater. Chem. A* **2015**, *3*, 18074–18082.
[46] H. Zhao, Y. Dong, P. Jiang, G. Wang, J. Zhang, *ACS Appl. Mater. Interfaces* **2015**, *7*, 6451–6461.
[47] Z. Li, Q. Gao, H. Zhang, W. Tian, Y. Tan, W. Qian, Z. Liu, *Sci. Rep.* **2017**, *7*, 43352.
[48] U. T. Bornscheuer, G. W. Huisman, R. J. Kazlauskas, S. Lutz, J. C. Moore, K. Robins, *Nature* **2012**, *485*, 185–194.
[49] J. Lehr, B. E. Williamson, F. Barriere, A. J. Downard, *Bioelectrochemistry* **2010**, *79*, 141–146.
[50] J. Shi, Z. Jiang, *J. Mater. Chem. B* **2014**, *2*, 4435–4441.
[51] G. C. V. Bittner, C. R. Bertozzi, C. J. Chang, *J. Am. Chem. Soc.* **2013**, *135*, 1783–1795.
[52] W. Wu, T. Zhou, A. Berliner, P. Banerjee, S. Zhou, *Angew. Chem. Int. Ed.* **2010**, *49*, 6554–6558; *Angew. Chem.* **2010**, *122*, 6704–6708.
[53] Q. Yuan, Y. Zhang, T. Chen, D. Lu, Z. Zhao, X. Zhang, Z. Li, C. H. Yan, W. Tan, *ACS Nano* **2012**, *6*, 6337–6344.

10.1002/chem.201703833

FULL PAPER

Text for Table of Contents

A novel peroxidase-mimicking nanozyme with enhanced activity and excellent stability was created by adopting a structural design approach through hybridization of cube-CeO_2 and Pt nanoparticles. This nanozyme can be used to construct high-performance colorimetric biosensors for the sensitive detection of metabolites including H_2O_2 and glucose, holding great promise in diagnostics and biomedicine.

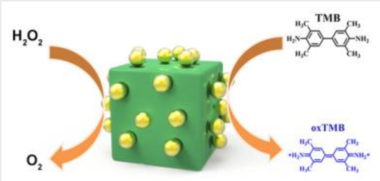

*Zhihao Li, Xiangdong Yang, Yanbing Yang, Yaning Tan, Yue He, Meng Liu, Xinwen Liu, Quan Yuan**

Page No.1 – Page No.7

Peroxidase-Mimicking Nanozyme with Enhanced Activity and High Stability based on Metal-Support Interaction